CHAPTER 5

Drosophila phosphopantothenoylcysteine synthetase is required for tissue morphogenesis during oogenesis

Floris Bosveld, Anil Rana, Willy Lemstra, Harm H. Kampinga, Ody C. M. Sibon

Department of Cell Biology, Section of Radiation & Stress Cell Biology,
University Medical Center Groningen, University of Groningen,
The Netherlands

BMC Research Notes 2008, 1:75

ABSTRACT

Background: Coenzyme A (CoA) is an essential metabolite, synthesized from vitamin B5 by the subsequent action of five enzymes: PANK, PPCS, PPCDC, PPAT and DPCK. Mutations in *Drosophila* d*PPCS* disrupt female fecundity and in this study we analyzed the female sterile phenotype of d*PPCS* mutants in detail.

Results: We demonstrate that d*PPCS* is required for various processes that occur during oogenesis including chorion patterning. Our analysis demonstrates that a mutation in *dPPCS* disrupts the organization of the somatic and germ line cells, affects F-actin organization and results in abnormal PtdIns(4,5)P2 localization. Improper cell organization coincides with aberrant localization of the membrane molecules Gurken (Grk) and Notch, whose activities are required for specification of the follicle cells that pattern the eggshell. Mutations in d*PPCS* also induce alterations in scutellar patterning and cause wing vein abnormalities. Interestingly, mutations in *dPANK* and *dPPAT-DPCK* result in similar patterning defects.

Conclusion: Together, our results demonstrate that *de novo* CoA biosynthesis is required for proper tissue morphogenesis.

INTRODUCTION

Coenzyme A (CoA), the major acyl carrier in all organisms, constitutes an essential cofactor to support cellular metabolism [1]. Synthesis of CoA occurs via a conserved route in which vitamin B5 is subsequently modified by five enzymes: PANK, PPCS, PPCDC, PPAT and DPCK [2-5]. Although CoA biosynthesis is well characterized in bacteria and in in vitro systems [6], only recently has the impact of abnormal CoA biosynthesis on animals been investigated [7-10].

Mutations in d*PPCS* impair female fecundity and fertility

Previously, we isolated a *Drosophila* d*PPCS* mutant as a female sterile, neurologically impaired mutant and we demonstrated that CoA metabolism is required to maintain DNA integrity during development of the central nervous system [8]. Here, we analyzed the female sterile phenotype of a hypomorphic allele of d*PPCS* (d*PPCS*^{1}) in detail. d*PPCS*^{33} mutants (a null allele) are homozygous lethal [8], and in d*PPCS*$^{1/33}$ mutants, no vitellogenic egg chambers were observed. Using immunohistochemistry and confocal laser scanning microscopy (supplement) we have analyzed the defects that occur during oogenesis (see for recent reviews [11,12]).

At 48 h after eclosion (AE), the ovaries from d*PPCS*$^{1/1}$ females were small compared to wild-type (wt) ovaries and mutant ovaries did not contain mature eggs (Fig. 1Aa-b). In wt, the oldest egg chambers found in newly eclosed females are at stage 7, and upon food intake, hormones are produced which trigger the egg chambers to proceed into vitellogenesis, a process whereby the oocyte accumulates nutrients and increases in size [13]. At 72 h AE, 100% (n=35) of the wt ovaries contained vitellogenic egg chambers, while only 11% of the d*PPCS*1/1 ovaries (n=36) contained vitellogenic egg chambers (Fig. 1Ac-d). At 120 h AE, 80% of the d*PPCS*$^{1/1}$ ovaries (n=26) contained vitellogenic egg chambers; however, the two lobes were frequently different in size and displayed features of degenerating egg chambers (Fig. 1Ae).

Between 144-192 h AE, d*PPCS*$^{1/1}$ females deposited 0.03 (± 0.02 SEM) eggs/24 h, none of which hatched (n=142 eggs), while wt females produced 10.0 (± 1.4 SEM) eggs/24 h, of which 90% hatched (n=1005 eggs). It has been reported that a mid-oogenesis checkpoint monitors the integrity of pre-vitellogenic egg chambers, and that activation of this checkpoint results in the removal of abnormal egg chambers [13]. A Tunnel assay was performed, which revealed that in d*PPCS*1/1 ovaries at 144 h AE, prior to vitellogenesis, a 6-fold increase of ovariols containing apoptotic egg chambers was observed, compared to wt ovaries (see additional file 1). Approximately 32% of d*PPCS*$^{1/1}$ ovariols (n=222) contained stage 5-7 egg chambers that displayed packaging defects (abnormal amount of germ line cells), while 4% of the wt ovariols (n=109) contained egg chambers with packaging defects. When we expressed a *dPPCS* transgene (P[d*PPCS*]) in the d*PPCS*$^{1/1}$ background, 11% (n=166) of the

ovariols displayed defects, demonstrating that d*PPCS* is required for early egg chamber development. Within d*PPCS*$^{1/1}$ germaria, aberrant separation of the developing egg chambers by the intercyst cells likely results in production of egg chambers with abnormal interfollicular stalk cell and/or polar follicle cell formation, egg chambers with mispositioned oocytes, or egg chambers that display packaging defects (see additional file 1). Thus, the reduced fecundity of the d*PPCS*$^{1/1}$ females is most likely due to production of aberrant egg chambers that did not pass the mid-oogenesis checkpoint and were absorbed.

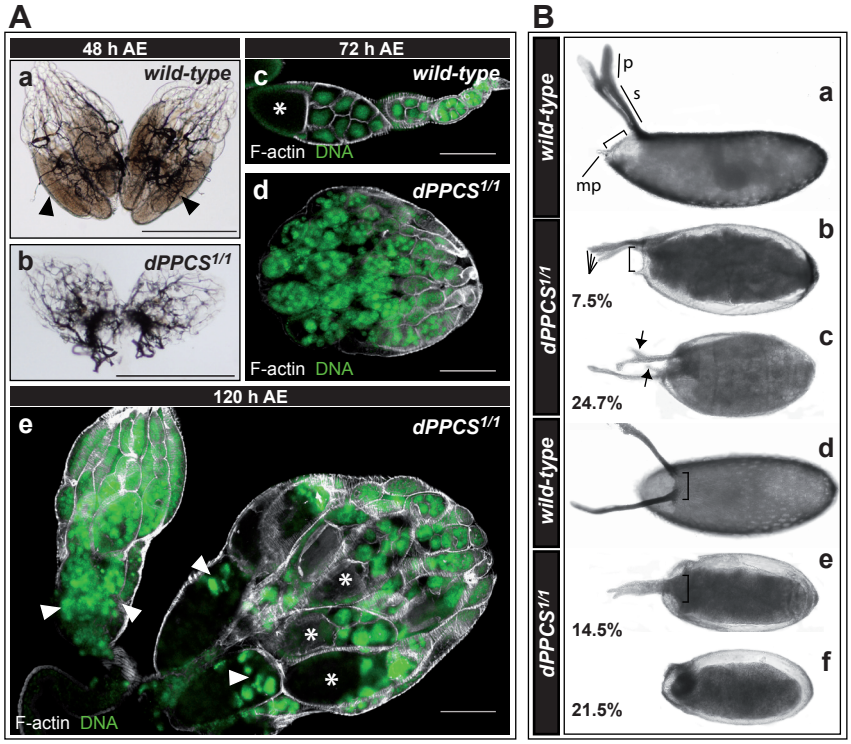

Figure 1. Egg chamber development and eggshell patterning is disrupted in d*PPCS*1/1
(A) dPPCS1/1 ovaries as compared with wt using light microscopy. (Aa) Bright field microscopy revealed that at 48 h after eclosion (AE), Wt ovaries are well developed & contain mature eggs (arrowheads). (Ab) At 48 h after eclosion, dPPCS1/1 ovaries were small in size compared to wt. (Ac-e) Ovaries with rhodamin-phalliodin to detect F-actin & DAPI to visualize DNA. (Ac) At 72 h AE, wt ovaries contain vitellogenic egg chambers, as determined by the increased size of the oocyte compartment (asterisk). (Ad) dPPCS1/1 ovaries remained small in size and no vitellogenic egg chambers were observed. (Ae) At 120 h AE, dPPCS1/1 ovaries contained vitellogenic egg chambers (*) & exhibited features of degenerating egg chambers (arrowheads). The 2 lobes were frequently different in size. (B) Chorion patterning was analysed in dPPCS1/1. (Ba, Bd) Wt embryos have 2 dorsal appendages. (mp = micropyle; p = paddle; s = stalk). (Bb-c, Be-f) Embryos deposited by dPPCS1/1 mothers showed a dumpless phenotype and had a wide range of patterning defects, which were classified in 5 groups: (Bb) embryos with opercula positioned in a different angle in relation to the stalks (bracket, compare with Ba) and 4 appendages; (Bc) abnormal stalks (arrows); (Be) fused appendages (bracket, compare with Bd); and (Bf) embryos without dorsal appendages. % are indicated (n=142). The remaining 22.8% had either 2 dorsal appendages of different lengths, missing paddles, or a shift of the dorsal appendages posteriorly. Scale bars: 500 µm (Aa-b), 150 µm (Ac-e).

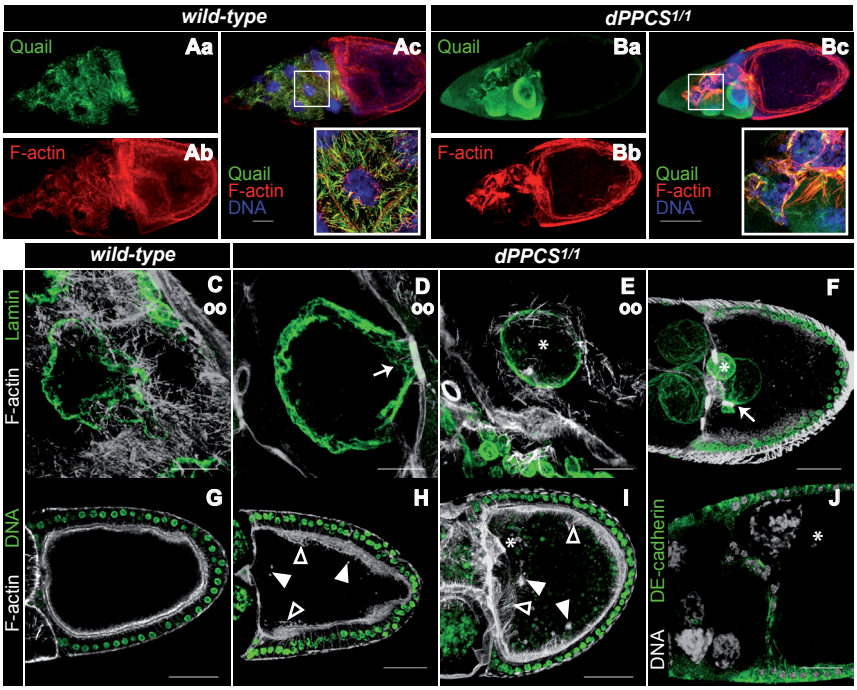

Figure 2. Cytoplasmic F-actin filament assembly and dumping is disrupted in d*PPCS*1/1 egg chambers
To examine the morphology of dPPCS1/1 mutant ovaries, rhodamin-phalloidin was used to visualize the F-actin network in combination with DAPI to stain nuclei and various other antibodies as described. (Aa-Ac) Wt nurse cells assemble an elaborate network of transverse F-actin filaments prior to cytoplasmic dumping. Labeling using antibodies against Quail revealed colocalization of Quail with F-actin filaments in wt. (Ba-Bc) The cytoplasmic F-actin network is not properly formed inside dPPCS1/1 nurse cells, and Quail localization is diffuse inside the cytoplasm. To visualize nurse cell nuclei an antibody against lamin Do was used. (C) In wt ovaries, F-actin bundles anchor the nurse cell nuclei during dumping. (D) dPPCS1/1 nurse cells fail to assemble F-actin filaments, and nurse cell nuclei trapped inside the ring canals during dumping were observed (arrows in D, F). (E) Example of a dPPCS1/1 oocyte nucleus encapsulated by F-actin fibers. (F) In dPPCS mutant egg chambers, nurse cell nuclei were found inside the oocyte compartment (arrow marks a nurse cell nucleus trapped inside a ring canal). (G) During cytoplasmic dumping, a tight array of F-actin is present at the subcortical membrane of wt oocytes. (H-I) The subcortical F-actin fibers at the membrane of the dPPCS1/1 oocyte compartment were increased in size and thickness (boxed arrowhead), and large clumps of F-actin were found within the oocyte compartment (arrowheads). (J) An antibody against DE-cadherin was used to visualize centripetal migrating follicle cells because these cells express high levels of DE-cadherin. In dPPCS mutants, migration of these cells occurred normally, but nurse cells are observed within the oocyte compartment after these cells finished their migration. An example of a nurse cell nucleus in the dorsoanterior corner of the dPPCS1/1 oocyte compartment is shown. Asterisks mark the oocyte nuclei. (oo) oocyte compartment. Scale bars: 100 µm (A-B), 20 µm (C-E), 50 µm (F-J).

d*PPCS is* required for F-actin remodeling during cytoplasmic dumping

In addition to impaired fecundity, 80% of the eggs deposited by d*PPCS*$^{1/1}$ females displayed a dumpless phenotype [14] and a wide array of chorion patterning defects (Fig. 1B). Since patterning defects can arise from aberrant actin fiber formation within the nurse cells

[15,16], we analyzed actin formation during cytoplasmic dumping. In stage 10 wt egg chambers, an elaborate network of F-actin bundles is assembled inside the nurse cells which is a prelude to cytoplasmic dumping. These bundles anchor the nurse cell nuclei to prevent them from entering the oocyte when the remaining nurse cell material is actively squeezed into the oocyte [17]. Assembly of this F-actin network requires the Quail protein, which colocalizes with the F-actin fibers (Fig. 2A) [16,18]. In d*PPCS*$^{1/1}$ egg chambers, assembly of the cytoplasmic F-actin fibers was disrupted, and the Quail protein failed to associate with the F-actin bundles and remained diffuse throughout the nurse cell cytoplasm (Fig. 2B). As a result of aberrant F-actin assembly, nurse cell nuclei were trapped inside ring canals during dumping (Fig. 2D, Table 1). Interestingly, we also found oocyte nuclei that were encapsulated by bundles of actin (Fig. 2E, Table 1). Furthermore, large actin fibers were assembled at the cortical membrane of the oocyte, and the follicular epithelium of the oocytes was frequently disorganized (Fig. 2H-I).

Table 1: Mutations in dPPCS affect egg chamber development, stage 10–11 F-actin organization & cytoplasmic dumping

	% of egg chambers		
	wild-type	**dPPCS1/1**	**P[dPPCS];dPPCS1/1**
Nurse cells trapped inside the oocyte	0.0 (n = 100)	20.9 (n = 67)	1.8 (n = 56)
F-actin clumps in ooplasm	3.0 (n = 100)	50.1 (n = 53)	7.0 (n = 57)
Aberrant F-actin in nurse cells	0.0 (n = 100)	92.2 (n = 51)	29.5 (n = 61)
Nurse cells plugging ring canals	0.0 (n = 100)	71.0 (n = 62)	15.5 (n = 58)
Oocytes with disorganized subcortical F-actin	0.0 (n = 100)	43.7 (n = 55)	0.0 (n = 53)
Oocyte nuclei with F-actin fibers	0.0 (n = 100)	18.8 (n = 48)	0.0 (n = 46)

Nurse cells were stained with DAPI to detect DNA and labeled with rhodamin-phalloidin to visualize the F-actin network. P[dPPCS] is a FLAG-tagged dPPCS cDNA under control of a ubiquitin promoter.

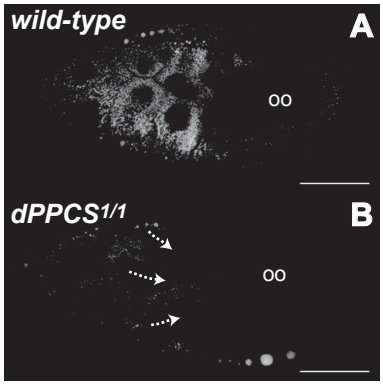

Figure 3. Synthesis and transport of neutral lipids is hampered in *dPPCS* mutant egg chambers

Freshly dissected wt and dPPCS$^{1/1}$ ovaries were stained with Nile red to visualize neutral lipids and dissected ovaries were directly analyzed by CLSM. Images represent single confocal scans. (A) Wt nurse cells produce high levels of neutral lipids, which are transported towards the oocyte, and are uniformly accumulated near the oocyte membrane. (B) dPPCS$^{1/1}$ nurse cells produced less neutral lipids compared to wt nurse cells. No uniformly accumulated lipids were observed within the mutant oocyte compartment compared to wt. (oo) oocyte compartment. Scale bars: 100 µm.

Mutant oocytes also contained large clumps of F-actin (Fig. 2H-I, Table 1) and we frequently found nurse cell nuclei inside the oocyte compartment (Fig. 2F, J, Table 1). We stained freshly dissected ovaries with Nile red, which has fluorescent properties in the presence of triacylglycerol and sterol esters [19], to determine if neutral lipid synthesis and transport of these lipids to the oocyte was disrupted during cytoplasmic dumping. In wt, synthesis of these neutral lipids increases in the germ line and somatic cells when egg chambers proceed into late stage oogenesis, and these neutral lipids are transported to the oocyte where they accumulate uniformly near the oocyte membrane (Fig. 3A). In d*PPCS*$^{1/1}$ egg chambers, neutral lipid synthesis was reduced compared to wt, suggesting that the synthesis of neutral lipids is affected in d*PPCS* mutants (Fig. 3B). Furthermore, accumulation inside the oocyte of these lipids appeared abnormal compared to wt ovaries (compare Fig. 3A and 3B).

Next, we investigated whether a mutation in *dPPCS*$^{1/1}$ affects cell migration events due to defective F-actin organization. During stages 8-10, the border cells, which include the anterior polar cells and part of the main body epithelium, migrate through the nurse cell compartment towards the anterior end of the oocyte [20]. In wt, when the border cells reach the oocyte and the centripetal follicle cells start migrating, Fasciclin III (FasIII) is expressed in the follicle cells of the dorsoanterior corner (Fig 4A). After centripetal follicle cells finished their migration, FasIII expressing cells form two distinct cell populations at the dorsoanterior surface of the oocyte. Here, formation of the dorsal appendages is initiated (Fig 4B) [14]. In d*PPCS*$^{1/1}$ egg chambers, centripetal migration was finished before the border cells reached the anterior of the oocyte (Fig 4C), indicating that these two cell migration events are not properly synchronized. Together, these data demonstrate that d*PPCS* is required for F-actin organization and cell migration events during oogenesis.

Grk and Notch localization is disrupted in dPPCS$^{1/1}$egg chambers

We hypothesized that disorganized tissue integrity may also affect the signaling routes required for specification of follicle cells that pattern the chorion. To investigate this, we stained ovaries with antibodies against Notch and Grk, which both are required for specification of the follicle cell populations that pattern the eggshell [14,21]. Although we cannot conclude that Grk or Notch signaling was disrupted in d*PPCS*$^{1/1}$ ovaries, the localization of both proteins was frequently impaired compared to wt ovaries. In wt egg chambers, when the border cells reach the centripetal follicle cells, Notch is highly expressed at the dorsoanterior corner, where it is required for the specification of the dorsal appendage producing cells, while Notch expression is restricted to the nurse cell membranes during cytoplasmic dumping (Fig. 4Ba, see additional file 1) [22]. In d*PPCS*$^{1/1}$ stage 11 egg chambers, Notch localization was more diffuse throughout the nurse cells and not restricted to the membranes (Fig. 4Ca). Notch localization was also severely affected during late stage oogenesis (see additional file 1) and FasIII staining revealed that the dorsal appendage/operculum forming follicle cells were not properly organized (see additional file 1).

In wt stage 9-10 egg chambers, Grk is localized at the dorsoanterior corner of the oocyte

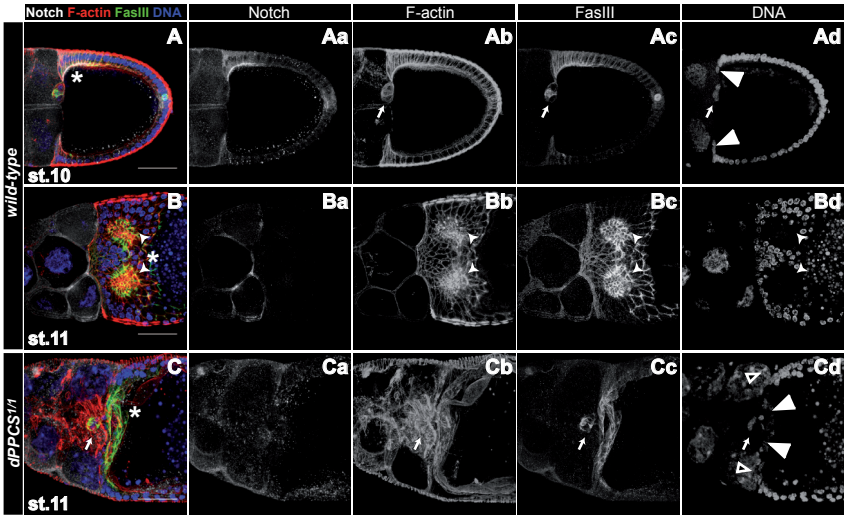

Figure 4. A mutation in d*PPCS* affect follicle cell migration and patterning

dPPCS1/1 and wt egg chambers were stained with rhodamin falloidin (to visualize F-actin) and DAPI to stain nuclei and labeled with antibodies against FasIII and Notch to analyze follicle cell migration and patterning. (Aa-Ad) Wt stage 10 egg chamber. During stages 8-10, the border cells migrate through the nurse cell compartment towards the anterior end of the oocyte. When the border cells (arrow) reach the oocyte (stage 10) and the centripetal follicle cells start migrating (arrowheads), FasIII is expressed in the follicle cells of the dorsoanterior corner. At this stage, Notch is expressed at the membranes of the follicle cells of the dorsoanterior corner, where it is required for the specification of the dorsal appendage producing cells. (Ba-Bd) During stage 11, after the centripetal cells finished their migration, two patches of follicle cells can be found at the dorsoanterior corner of the epithelium of wt egg chambers (arrowheads). These follicle cells express high levels of FasIII and will initiate the production of the dorsal appendages. At this stage, Notch expression is restricted to the nurse cell membranes. (Ca-Cd) dPPCS1/1 egg chamber at stage 11. The centripetal follicle cells finished migration (arrowheads), but the border cells (arrow) failed to reach the centripetal follicle cells, while follicle cells of the dorsoanterior corner were already expressing FasIII. The border cell cluster is surrounded by an elaborate network of F-actin. Notch localization is not restricted to the nurse cell membranes and shows a more diffuse pattern. Boxed arrowheads point to two nurse cell nuclei that seem to contact (push against) the centripetal follicle cells. Asterisks mark the position of the oocyte. Scale bars: 50 μm.

Figure 5. PtdIns(4,5)P2 localization and expression is affected in d*PPCS*1/1

We overexpressed a PLCδ-PH-GFP fusion protein [25] under the control of a ubiquitously expressed Act5C-GAL4 driver to analyze PtdIns(4,5)P2 localization and expression in a wt (A,B,E,G) and dPPCS1/1 (C,D,F,H) background. (A,B) During wt oogenesis, the PLCδ-PH-GFP fusion protein is present at the border cells (asterisk) and the apical membranes of the follicle cells that encapsulate the oocyte compartment, while the nurse cell membranes do not accumulate the fusion protein. (C,D) In dPPCS1/1 egg chambers, the PLCδ-PH-GFP fusion protein is not present at the apical membranes of the follicle cells that encapsulate the oocyte (arrowheads) and large patches of follicle cells are not labeled (dashed lines). In mutant ovaries, the follicular epithelium is sometimes disrupted (arrows in C), and the nurse cell membranes accumulate patches of high levels of the PLCδ-PH-GFP fusion protein (arrow in D). The PLCδ-PH-GFP fusion protein was also frequently detected at membranes of cells that are (based on their localization) most likely border cells (boxed arrowhead in D). (E-H) For further analysis, F-actin organization was analyzed in combination with localization of the PLCδ-PH-GFP fusion protein. (Ea-Ec) In wt egg chambers, the oocyte cortex is in close contact with the apical membranes of the follicle cells, which accumulate the PLCδ-PH-GFP fusion protein.

(F) In dPPCS1/1 egg chambers, the oocyte cortex is disrupted (arrowheads in Fa) and the follicle cells do not accumulate the PLCδ-PH-GFP fusion protein (arrowheads and dashed lines in Fb). Arrows point to defects in cell organization of the follicular epithelium. (G) Higher magnification of a wt egg chamber, showing that the PLCδ-PH-GFP fusion protein accumulates at the apical membranes of follicle cells in close contact with the oocyte cortex (boxed arrowheads). (H) Higher magnification of a dPPCS1/1 egg chamber, showing that the apical membranes of follicle cells in close contact with the oocyte cortex do not accumulate the PLCδ-PH-GFP fusion protein (arrowheads in Ha). This coincides with impaired oocyte cortex morphology and aberrant F-actin nucleation (arrow in Hb). DAPI was used to visualize DNA. Scale bars: 150 μm (A,C), 100 μm (B,D), 50 μm (E-H).

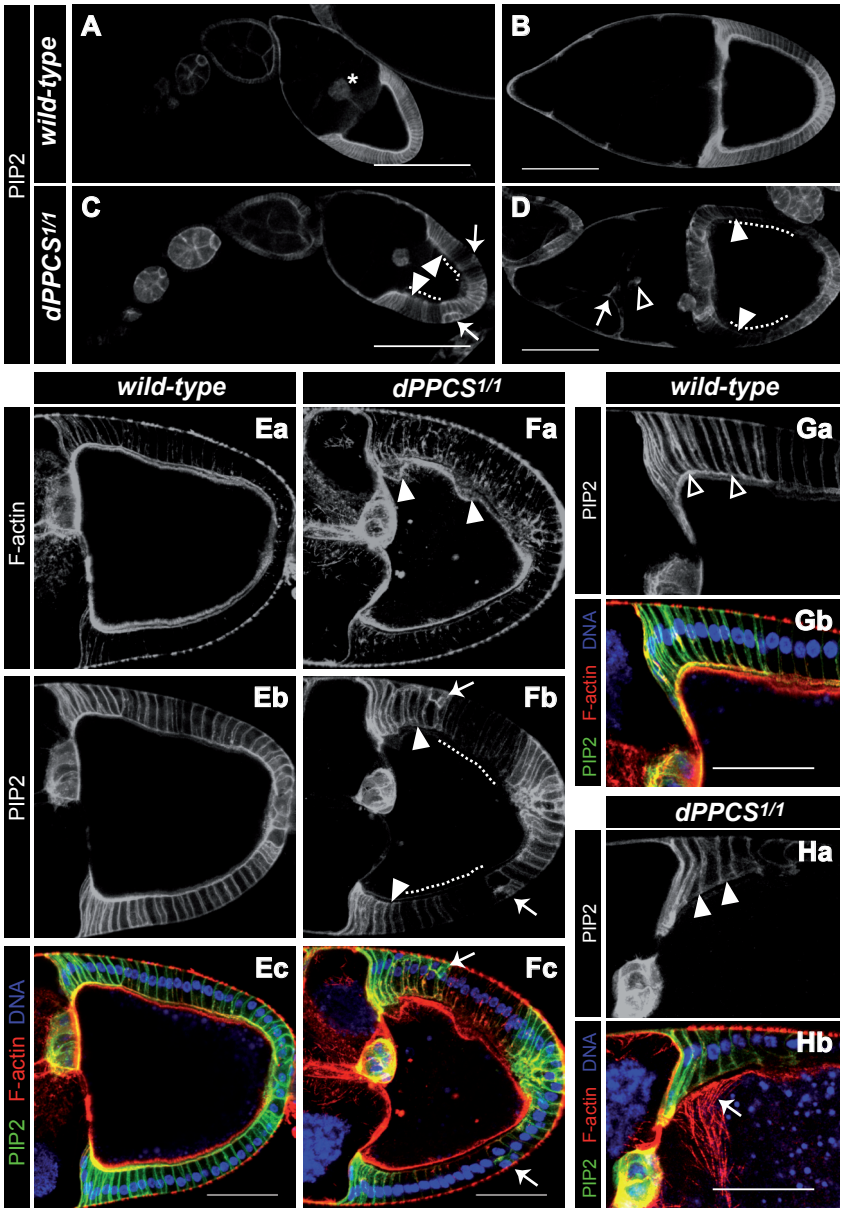

compartment. Although in d*PPCS*$^{1/1}$ egg chambers, Grk was present at the dorsoanterior corner, the distribution of the protein was frequently impaired in stage 8-9 egg chambers (see additional file 1) and progressively worsened when egg chambers proceeded into later stages of oogenesis (see additional file 1).

These findings imply that d*PPCS* is not required for cell specification or signaling per se, but merely required for cell organization and morphology. This is supported by the finding that aberrant intercyst cell migration/organization likely underlies the observed packaging and follicle cell specification defects during early oogenesis (see additional file 1).

Membrane localization of PtdIns(4,5)P2 is impaired in *dPPCS*$^{1/1}$

The levels of phospholipids are reduced in d*PPCS* mutant flies, indicating a general defect in phospholipid biosynthesis [8]. Therefore, it is plausible to assume that phosphatidylinositol (PtdIns) production, the precursor for all phosphoinositides [23], is also reduced. Although levels and localization of PtdIns have not been determined during *Drosophila* oogenesis, it is generally accepted that actin remodeling processes depend on PtdIns signaling [24].

To investigate whether PtdIns signaling was affected in *dPPCS* mutant ovaries, we expressed a PLCδ-PH-GFP fusion protein, which is able to bind to PtdIns(4,5)P2 [25]. We used an Act5C-GAL4 driver to analyze PLCδ-PH-GFP expression and thus PtdIns(4,5)P2 localization in all cells. During wt cytoplasmic dumping, PtdIns(4,5)P2 is abundant at the cell membranes of the border cells and the apical membranes of the follicle cells that encapsulate the oocyte, while low levels of PtdIns(4,5)P2 can be detected at the nurse cell membranes (Fig. 5A,B,E). In contrast, PtdIns(4,5)P2 localization at the apical membranes of the follicle cells that encapsulate the oocyte was hardly detectable or absent in d*PPCS*$^{1/1}$ egg chambers (Fig. 5C,D,F,H). Moreover, large patches of follicle cells that encapsulate the oocyte did not accumulate PtdIns(4,5)P2 at their membranes (Fig. 5C,D,F). Because aberrant apical localization of PtdIns(4,5)P2 at the follicle cell membranes coincides with impaired oocyte cortex integrity and abnormal F-actin organization (Fig. 5H), this suggests that altered PtdIns(4,5)P2 signaling could underlie the F-actin defects in d*PPCS*$^{1/1}$ egg chambers.

Although the F-actin/PtdIns(4,5)P2 connection should be investigated in more detail, we propose that F-actin remodeling within the *Drosophila* ovary likely depends on PtdIns(4,5)P2 signaling and that this lipid derived signaling route is disrupted in d*PPCS*$^{1/1}$. Abnormal cytoskeletal organization in d*PPCS*$^{1/1}$ disrupts the overall shape of all membranous structures and the organization of the cells during morphogenesis. Disorganized tissue integrity could affect Notch and Grk localization and possibly signaling, which is required for specification of the follicle cells that pattern the eggshell, and causes severe chorion patterning defects.

dPPCS is required for patterning of various tissues

Next, we wondered whether ***dPPC****S* is also required for morphogenesis of other tissues. Hereto, we closely investigated *dPPCS*$^{1/1}$ flies for other morphological abnormalities. A stereotypical pattern of four scutellars exists on the dorsal surface of the wt scutellum, and d*PPCS* mutants displayed ectopic formation of scutellars (see additional file 1). Furthermore, d*PPCS1/1* flies also developed ectopic wing veins (see additional file 1). Mutants initiated longitudinal vein formation between L3-L4 and L4-L5. These results show that d*PPCS* is required for morphogenesis of various tissues during *Drosophila* development.

Mutations in *de novo* CoA synthesis disrupt morphogenesis

Next, we investigated whether mutations in other CoA biosynthesis enzymes give rise to similar defects. Indeed, mutations in *dPANK*/*fumble* and the bifunctional enzyme *dPPAT-DPCK* result in similar characteristics compared to the d*PPCS* mutant phenotype. *dPANK/fumble* and *dPPAT-DPCK* mutant females have poorly developed ovaries, have fecundity defects, produce eggs that exhibit polarity defects, synthesize abnormal neutral lipids (droplets), and these mutants display scutellar and wing vein patterning defects (see additional file 1). As in d*PPCS*$^{1/1}$, a mutation in *dPPAT-DPCK* disrupts actin localization and results in plugging of the ring canals by nurse cell nuclei during dumping (see additional file 1). *dPANK*/*fumble* mutants produce small ball-shaped eggs, which are typically due to a loss of actin regulatory elements that control the polarized arrangement of F-actin fibers at the basal cortex of follicle cells required to establish planar cell polarity [11]. These findings imply that impaired CoA synthesis in general disrupts morphogenesis, possibly due to aberrant F-actin organization. Because the biosynthesis route towards the production of CoA is conserved amongst species it would be interesting to explore the significance of CoA during processes that involve actin/PtdIns dynamics such as chemotaxis, axon growth cone guidance, endocytosis/exocytosis, cell division or actin dependent chromatin remodeling.

ACKNOWLEDGMENTS

We thank L. Cooley and A. Wodarz for the UAS-PLCδ-PH-GFP line and S. Wasserman for the P[dPANK] line. This work was supported by a VIDI grant from the Netherlands Organization for Scientific Research (NWO; 971-36-400) to O.C.M.S and by a Topmaster grant from the Graduate School GUIDE to A.R.

REFERENCES

1. Begley TP, Kinsland C, Strauss E: The biosynthesis of coenzyme A in bacteria. Vitam Horm 2001, 61: 157-171.

2. Strauss E, Kinsland C, Ge Y, McLafferty FW, Begley TP: Phosphopantothenoylcysteine synthetase from Escherichia coli. Identification and characterization of the last unidentified coenzyme A biosynthetic enzyme in bacteria. J Biol Chem 2001, 276: 13513-13516.

3. Genschel U: Coenzyme A biosynthesis: reconstruction of the pathway in archaea and an evolutionary scenario based on comparative genomics. Mol Biol Evol 2004, 21: 1242-1251.

4. Kupke T, Hernandez-Acosta P, Culianez-Macia FA: 4'-phosphopantetheine and coenzyme A biosynthesis in plants. JBC 2003, 278: 38229-38237.

5. Daugherty M, Polanuyer B, Farrell M, Scholle M, Lykidis A, Crecy-Lagard V et al.: Complete reconstitution of the human coenzyme A biosynthetic pathway via comparative genomics. J Biol Chem 2002, 277: 21431-21439.

6. Leonardi R, Zhang YM, Rock CO, Jackowski S: Coenzyme A: back in action. Prog Lipid Res 2005, 44: 125-153.

7. Afshar K, Gonczy P, DiNardo S, Wasserman SA: *fumble* encodes a pantothenate kinase homolog required for proper mitosis and meiosis in *Drosophila* melanogaster. Genetics 2001, 157: 1267-1276.

8. Bosveld F, Rana A, van der Wouden PE, Lemstra W, Ritsema M, Kampinga HH et al.: *De novo* CoA biosynthesis is required to maintain DNA integrity during development of the *Drosophila* nervous system Hum Mol Genet 2008, 17: 2058-69.

9. Kuo YM, Duncan JL, Westaway SK, Yang H, Nune G, Xu EY et al.: Deficiency of pantothenate kinase 2 (Pank2) in mice leads to retinal degeneration and azoospermia. HumMol Genet 2005, 14: 49-57.

10. Zhou B, Westaway SK, Levinson B, Johnson MA, Gitschier J, Hayflick SJ: A novel pantothenate kinase gene (PANK2) is defective in Hallervorden-Spatz syndrome. Nat Genet 2001, 28: 345-349.

11. Horne-Badovinac S, Bilder D: Mass transit: epithelial morphogenesis in the *Drosophila* egg chamber. Dev Dyn 2005, 232: 559-574.

12. Lopez-Schier H: The polarisation of the anteroposterior axis in *Drosophila*. Bioessays 2003, 25: 781-791.

13. Drummond-Barbosa D, Spradling AC: Stem cells and their progeny respond to nutritional changes during *Drosophila* oogenesis. Dev Biol 2001, 231: 265-278.

14. Berg CA: The *Drosophila* shell game: patterning genes and morphological change. Trends Genet 2005, 21: 346-355.

15. Cant K, Knowles BA, Mooseker MS, Cooley L: *Drosophila* singed, a fascin homolog, is required for actin bundle formation during oogenesis and bristle extension. J Cell Biol 1994, 125: 369-380.

16. Mahajan-Miklos S, Cooley L: The villin-like protein encoded by the *Drosophila* quail gene is required for actin bundle assembly during oogenesis. Cell 1994, 78: 291-301.

17. Hudson AM, Cooley L: Understanding the function of actin-binding proteins through genetic analysis of *Drosophila* oogenesis. Annu Rev Genet 2002, 36: 455-488.

18. Matova N, Mahajan-Miklos S, Mooseker MS, Cooley L: *Drosophila* quail, a villin-related protein, bundles actin filaments in apoptotic nurse cells. Development 1999, 126: 5645-5657.

19. Greenspan P, Mayer EP, Fowler SD: Nile red: a selective fluorescent stain for intracellular lipid droplets. J Cell Biol 1985, 100: 965-973.

20. Rorth P: Initiating and guiding migration: lessons from border cells. Trends Cell Biol 2002, 12: 325-331.

21. Ward EJ, Zhou X, Riddiford LM, Berg CA, Ruohola-Baker H: Border of Notch activity establishes a boundary between the two dorsal appendage tube cell types. Dev Biol 2006, 297: 461-470.

22. Xu T, Caron LA, Fehon RG, Artavanis-Tsakonas S: The involvement of the Notch locus in *Drosophila* oogenesis. Development 1992, 115: 913-922.

23. Imai A, Gershengorn MC: Independent phosphatidylinositol synthesis in pituitary plasma membrane and endoplasmic reticulum. Nature 1987, 325: 726-728.

24. Logan MR, Mandato CA: Regulation of the actin cytoskeleton by PIP2 in cytokinesis. Biol Cell 2006, 98: 377-388.

25. von Stein W, Ramrath A, Grimm A, Muller-Borg M, Wodarz A: Direct association of Bazooka/PAR-3 with the lipid phosphatase PTEN reveals a link between the PAR/aPKC complex and phosphoinositide signaling. Development 2005, 132: 1675-1686.

ADDITIONAL FILE 1 - CHAPTER 5

Experimental procedures

***Drosophila* stocks:** Fly stocks were maintained at 22°C according to standard protocols. For wt preparations, y1w1118 was used. dPANK1 (*fumble*), dPPAT-DPCK43, d*PPCS*1, d*PPCS*33 and P[d*PPCS*] are previously described [1,2]. The UAS-PLCδ-PH-GFP line was a gift from L. Cooley and A. Wodarz and the Act5C-GAL4 line was obtained from the Bloomington Stock Centre (Indiana University, USA).

Immunohistochemistry: Dissection, fixation and immunolabeling of ovaries was performed as previously described [3]. Primary antibodies used included concentrated supernatants obtained from the Developmental Studies Hybridoma Bank (Iowa, USA), mouse anti-lamin Do (ADL84.12, 1:5) developed by P.A. Fisher, mouse anti-fasciclin III (7G10, 1:5) developed by C. Goodman, mouse anti-Notch (C17.9C6, 1:5) developed by S. Artavanis-Tsakonas, mouse anti-quail (6B9, 1:5) developed by L. Cooley, mouse anti-DE-cadherin, (DCAD2, 1:5) developed by T. Uemura, mouse anti-gurken (1D12, 1:5) developed by T. Schupbach, mouse anti-orb (6H4, IgG2a, 1:5) developed by P. Schedl, mouse anti-armadillo (N27A1, IgG2a, 1:5) developed by E. Wieschaus, and mouse anti-Histone H3 pS10 (1:100, Cell Signaling). Rabbit anti-Vasa (1:50) was a kind gift of P. Lasko. Secondary antibodies included Cy3-conjugated goat anti-mouse (1:200, Jackson ImmunoResearch), FITC-conjugated goat anti-mouse (1:200, Jackson ImmunoResearch), Cy5-conjugated goat anti-mouse 1:200, Jackson ImmunoResearch) and Alexa 647 goat anti-mouse IgG2a (1:200, Molecular probes). Ovaries were stained with 20 U/ml rhodaminphalloidin (Molecular Probes) and 0.2 µg/ml DAPI (Sigma) to visualize F-actin and DNA, respectively. Apoptosis was measured in 6-d-old flies that were kept for 3 days in vials containing yeast paste. The TUNEL cell death assay was performed following the ApopTag Fluorescien In Situ Apoptosis Detection Kit (Chemicon). Ovaries were fixed in devitellizing buffer/heptane [3] (1:6 per volume) and pretreated with proteinase K (20 ug/ml in PBS + 0.1% Tween-20) for 15 min at room temperature. After labeling and washing, ovaries were mounted in citifluor (Agar Scientific), and analyzed by confocal laser scanning microscopy (CLSM) (Leica TCS SP2 DM RXE). Images represent maximal projections (unless otherwise noted) of a z-stack (0.5-1 µm/scan). Images were processed using Leica software and Paint Shop Pro. For Nile red (Sigma) staining 6-d-old flies were kept for 3 days in vials containing yeast paste. Ovaries were dissected and stained with 100 ng/ml Nile red solution in PBS for 5 min. Ovaries were washed 3 times for 10 min with PBS, mounted in citifluor and directly analyzed by CLSM.

Assessment of fecundity and morphological analyses: For studies of fecundity, 10 groups of 5 virgin females and 5 males were crossed for 5 days in vials containing yeast paste. Flies were transferred to fresh vials without yeast and transferred to fresh vials every 24 h. The average number of eggs deposited/24 h was calculated from 3 replicates of each group. To assay embryonic viability, embryos were collected (0-6 h) on apple juice plates

containing yeast paste, counted, and the hatch rate was determined by visual inspection of the egg cases two days after egg laying. Inspection of chorion morphology was carried out using LM. Images were captured with an Olympus BX50 light microscope. To analyze ovary morphology, virgin females were placed in vials containing yeast paste and ovaries were dissected 48 h, 72 h and 120 h AE. Ovaries dissected 48 h AE were directly analyzed by light microscopy (LM) (Olympus BX50), while ovaries dissected 72 h and 120 h AE were fixed, labeled and inspected by CLSM. Assessment of wing venation and sensory organ patterning was performed by LM.

SUPPLEMENTARY REFERENCES

1. Afshar K, Gonczy P, DiNardo S, Wasserman SA: encodes a pantothenate kinase homolog required for proper mitosis and meiosis in *Drosophila melanogaster*. Genetics 2001, 157: 1267-1276.

2. Bosveld F, Rana A, van der Wouden PE, Lemstra W, Ritsema M, Kampinga HH et al.: *De novo* CoA biosynthesis is required to maintain DNA integrity during development of the *Drosophila* nervous system. Hum Mol Genet 2008 17:2058-2069

3. Verheyen E, Cooley L: Looking at oogenesis. Methods Cell Biol 1994, 44: 545-561.

4. Bai J, Montell D: Eyes absent, a key repressor of polar cell fate during *Drosophila* oogenesis. Development 2002, 129: 5377-5388.

5. Margolis J, Spradling A: Identification and behavior of epithelial stem cells in the *Drosophila* ovary. Development 1995, 121: 3797-3807.

6. Tworoger M, Larkin MK, Bryant Z, Ruohola-Baker H: Mosaic analysis in the drosophila ovary reveals a common hedgehog-inducible precursor stage for stalk and polar cells. Genetics 1999, 151: 739-748.

7. Ruohola H, Bremer KA, Baker D, Swedlow JR, Jan LY, Jan YN: Role of neurogenic genes in establishment of follicle cell fate and oocyte polarity during oogenesis in *Drosophila*. Cell 1991, 6: 433-449.

8. Bilder D, Li M, Perrimon N: Cooperative regulation of cell polarity and growth by *Drosophila* tumor suppressors. Science 2000, 289: 113-116.

9. Grammont M, Irvine KD: fringe and Notch specify polar cell fate during *Drosophila* oogenesis. Development 2001, 128: 2243-2253.

10. Grammont M, Irvine KD: Organizer activity of the polar cells during *Drosophila* oogenesis. Development 2002, 129: 5131-5140.

11. Lopez-Schier H, St Johnston D: Delta signaling from the germ line controls the proliferation and differentiation of the somatic follicle cells during *Drosophila* oogenesis. Genes Dev 2001, 15: 1393-1405.

12. Torres IL, Lopez-Schier H, St Johnston D: A Notch/Delta-dependent relay mechanism establishes anterior-posterior polarity in *Drosophila*. Dev Cell 2003, 5: 547-558.

13. Brown EH, King RC: Studies on the events resulting in the formation of an egg chamber in *Drosophila melanogaster*. Growth 1964, 28: 41-81.

14. Hawkins NC, Thorpe J, Schupbach T: Encore, a gene required for the regulation of germ line mitosis and oocyte differentiation during *Drosophila* oogenesis. Development 1996, 122: 281-290.

15. O'Reilly AM, Ballew AC, Miyazawa B, Stocker H, Hafen E, Simon MA: Csk differentially regulates Src64 during distinct morphological events in *Drosophila* germ cells. Development 2006, 133: 2627-2638.

16. Lantz V, Chang JS, Horabin JI, Bopp D, Schedl P: The *Drosophila* orb RNA-binding protein is required for the formation of the egg chamber and establishment of polarity. Genes Dev 1994, 8: 598-613.

17. Hay B, Jan LY, Jan YN: Localization of vasa, a component of *Drosophila* polar granules, in maternal-effect mutants that alter embryonic anteroposterior polarity. Development 1990, 109: 425-433.

18. Jackson SM, Blochlinger K: cut interacts with

Notch and protein kinase A to regulate egg chamber formation and to maintain germline cyst integrity during *Drosophila* oogenesis. Development 1997, 124: 3663-3672.

19. Zhang Y, Kalderon D: Regulation of cell proliferation and patterning in *Drosophila* oogenesis by Hedgehog signaling. Development 2000, 127: 2165-2176.

20. Oh J, Steward R: Bicaudal-D is essential for egg chamber formation and cytoskeletal organization in drosophila oogenesis. Dev Biol 2001, 232: 91-104.

21. Besse F, Busson D, Pret AM: Fused-dependent Hedgehog signal transduction is required for somatic cell differentiation during *Drosophila* egg chamber formation. Development 2002, 129: 4111-4124.

22. Goode S, Melnick M, Chou TB, Perrimon N: The neurogenic genes egghead and brainiac define a novel signaling pathway essential for epithelial morphogenesis during *Drosophila* oogenesis. Development 1996, 122: 3863-3879.

23. Horne-Badovinac S, Bilder D: Mass transit: epithelial morphogenesis in the *Drosophila* egg chamber. Dev Dyn 2005, 232: 559-574.

24. Deng WM, Althauser C, Ruohola-Baker H: Notch-Delta signaling induces a transition from mitotic cell cycle to endocycle in *Drosophila* follicle cells. Development 2001, 128: 4737-4746.

25. Dej KJ, Spradling AC: The endocycle controls nurse cell polytene chromosome structure during *Drosophila* oogenesis. Development 1999, 126: 293-303.

26. King R.C.. Ovarian development in *Drosophila melanogaster*., Academic Press, New York, 1970.

27. Patel NH, Snow PM, Goodman CS: Characterization and cloning of fasciclin III: a glycoprotein expressed on a subset of neurons and axon pathways in *Drosophila*. Cell 1987, 48: 975-988.

28. Peifer M, Orsulic S, Sweeton D, Wieschaus E: A role for the *Drosophila* segment polarity gene armadillo in cell adhesion and cytoskeletal integrity during oogenesis. Development 1993, 118: 1191-1207.

29. Godt D, Tepass U: *Drosophila* oocyte localization is mediated by differential cadherin-based adhesion. Nature 1998, 395: 387-391.

30. Gonzalez-Reyes A, St Johnston D: The *Drosophila* AP axis is polarised by the cadherin-mediated positioning of the oocyte. Development 1998, 125: 3635-3644.

31. Mahowald AP, Strassheim JM: Intercellular migration of centrioles in the germarium of *Drosophila melanogaster*. An electron microscopic study. J Cell Biol 1970, 45: 306-320.

32. Lopez-Schier H: The polarisation of the anteroposterior axis in *Drosophila*. Bioessays 2003, 25: 781-791.

33. Xu T, Caron LA, Fehon RG, Artavanis-Tsakonas S: The involvement of the Notch locus in *Drosophila* oogenesis. Development 1992, 115: 913-922.

34. Duffy JB, Harrison DA, Perrimon N: Identifying loci required for follicular patterning using directed mosaics. Development 1998, 125: 2263-2271.

35. Bateman J, Reddy RS, Saito H, Van Vactor D: The receptor tyrosine phosphatase Dlar and integrins organize actin filaments in the *Drosophila* follicular epithelium. Curr Biol 2001, 11: 1317-1327.

36. Frydman HM, Spradling AC: The receptor-like tyrosine phosphatase lar is required for epithelial planar polarity and for axis determination within drosophila ovarianfollicles. Development 2001, 128: 3209-3220.

37. Gutzeit HO, Eberhardt W, Gratwohl E: Laminin and basement membrane-associated microfilaments in wild-type and mutant *Drosophila* ovarian-follicles. J Cell Sci 1991, 100 (Pt 4): 781-788.

38. Deng WM, Schneider M, Frock R, Castillejo-Lopez C, Gaman EA, Baumgartner S et al.: Dystroglycan is required for polarizing the epithelial cells and the oocyte in *Drosophila*.Development 2003, 130: 173-184.

39. Deng WM, Ruohola-Baker H: Laminin A is required for follicle cell-oocyte signaling that leads to establishment of the anterior-posterior axis in *Drosophila*. Curr Biol 2000, 10: 683-686.

40. Mahajan-Miklos S, Cooley L: The villin-like protein encoded by the *Drosophila* quail gene is required for actin bundle assembly during oogenesis. Cell 1994, 78: 291-301.

41. Gutzeit HO: The microfilament pattern in the somatic follicle cells of mid-vitellogenic ovari-

anfollicles of *Drosophila*. Eur J Cell Biol 1990, 53: 349-356.

42. Adler PN: Planar signaling and morphogenesis in *Drosophila*. Dev Cell 2002, 2: 525-535.

43. Vereshchagina N, Wilson C: Cytoplasmic activated protein kinase Akt regulates lipid-droplet accumulation in *Drosophila* nurse cells. Development 2006, 133: 4731-4735.

Packaging defect in *dPPCS1*/1 egg chambers are likely due to impaired intercyst cell behavior (Supplementary Fig. S1): Shows that d*PPCS*$^{1/1}$ germaria display: 1) incomplete follicle cell migration; 2) fusion of cysts; 3) aberrant formation of the interfollicular stalk that separates neighboring egg chambers; and 4) cysts in region 2b of the germarium that do not show the characteristic lens-shape, indicative of aberrant encapsulation of cysts. Furthermore, stage 3-6 d*PPCS*1/1 egg chambers with mispositioned oocytes show ectopic polar follicle cells and egg chambers are frequently present that are not separated by interfollicular stalk cells. In addition, egg chambers are present that are separated by elongated stalks containing undifferentiated follicle cells. Proper formation of these stalk cells is essential to ensure packaging of the egg chambers prior to budding from the germarium. Because the polar follicle and the stalk cell populations are derived from the intercyst cells [4-6], it is possible that packaging defects in d*PPCS*$^{1/1}$ are due to aberrant intercyst cell specification and/or organization [7-12]. Aberrant follicle cell specification/organization is supported by the finding that in d*PPCS*1/1 mutants, FasIII localization is also detected in stage 7 egg chambers, indicating that differentiation of the cuboidal follicle cells that encapsulate the egg chambers is sometimes disrupted. Moreover, d*PPCS*$^{1/1}$ egg chambers are present in which the follicle cells accumulate in a bilayer at the posterior of the oocyte and Notch is frequently abnormally localized in mutant germaria. In d*PPCS*1/1 mutants, egg chambers with supernumerary nurse cells and oocytes are present and the ratio of nurse cells to oocytes is not always 15:1. In addition, the mispositioned oocyte(s) (n >100) in d*PPCS*1/1 egg chambers do not have more than the normal amount of 4 ring canals [13], suggesting that supernumerary cells are not due to extra cell divisions with incomplete cytokinesis [14]. Similarly, supernumerary cells are also not the result of extra cell division with complete cytokinesis, because extra germ cells areaccompanied by extra ring canals [15]. d*PPCS*1/1 oocytes accumulate normal amounts of the Orb protein [16], and the germ line cells accumulate normal amounts of the Vasa protein [17]. Therefore, the observed supernumerary cells are not due to disrupted germ cell identity or oocyte specification.

Finally, no defects in follicle cell proliferation are present (no major gaps in the follicular epithelia we detected); therefore, the supernumerary nurse cells and oocytes are not a result of abnormal follicle cell proliferation [18-21]. Taken together, these analyses indicate that packaging defects in d*PPCS*1/1 females may result from abnormal cyst encapsulation and abnormal budding due to aberrant intercyst cell behavior and organization. Because we observed abnormal cyst development from region 2b onwards, we believe that d*PPCS* is required for normal encapsulation of the cyst by the intercyst cells [22]. Aberrant migratory behaviour or organization of the intercyst cells likely induces mislocalization of

the Armadillo (Arm), DE-cadherin (DE-cad) and Notch expressing follicle cells, which, in turn, disrupts differentiation of the stalk cells, the polar follicle cells and the cuboidal follicle cells. Concomitantly, cyst encapsulation, anteroposterior axis formation (germ line cell rearrangement) and budding of follicles is disrupted. Because the correct positioning of the germ line cells and the follicle cells in the germarium is largely driven by cytoskeletal rearrangements and changes in cell adhesion [23], it is also possible that a mutation in *dPPCS* affects cell organization/ migration by disrupting cytoskeletal remodeling due to changes in PtdIns homeostasis within the germarium.

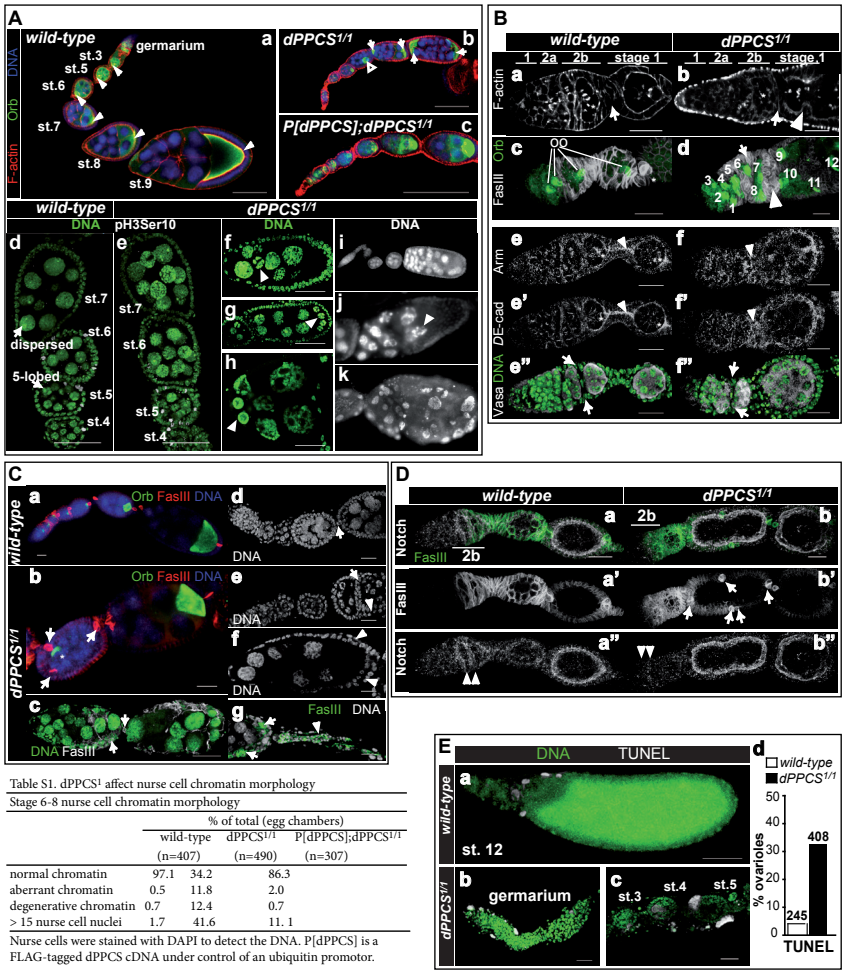

Table S1. dPPCS[1] affect nurse cell chromatin morphology

Stage 6-8 nurse cell chromatin morphology

	% of total (egg chambers)		
	wild-type (n=407)	dPPCS$^{1/1}$ (n=490)	P[dPPCS];dPPCS$^{1/1}$ (n=307)
normal chromatin	97.1	34.2	86.3
aberrant chromatin	0.5	11.8	2.0
degenerative chromatin	0.7	12.4	0.7
> 15 nurse cell nuclei	1.7	41.6	11. 1

Nurse cells were stained with DAPI to detect the DNA. P[dPPCS] is a FLAG-tagged dPPCS cDNA under control of an ubiquitin promotor.

Figure S1. d*PPCS*[1] affects germ line cell and follicle cell integrity during early oogenesis

Early oogenesis was investigated in dPPCS$^{1/1}$ ovaries and compared to wt. Antibodies against pH3Ser10 were used to detect mitotic chromatin. Several antibodies were used to visualize various structures and cell types. An-

ti-FasIII antibodies were used because FasIII is expressed in all undifferentiated follicle cells in the germarium and FasIII localization marks the polar follicle cells after the egg chambers bud from the germarium. Antibodies against Armadillo (Arm) and DE-cadherin (DE-cad) were used because Arm and DE-cad are expressed in the adhesive junctions of the migrating follicle cells that assist in the rearrangement of the germ line cells. Antibodies against Orb were used because Orb marks oocytes. Antibodies against Vasa were used because Vasa specifically accumulates inside germ line cells. DAPI was used to stain DNA, and rhodamin-phalloidin was used to visualize F-actin.

(A) dPPCS is required for nurse cell chromatin condensation, egg chamber packaging and polarity. (Aa) In wt egg chambers, Orb labeling reveals the wild type localization pattern of the oocytes (arrowheads). (Ab) dPPCS1/1 ovariols contain egg chambers with multiple (arrows) or mispositioned (arrowhead) oocytes. (Ac) Overexpression of a FLAG-tagged dPPCS cDNA (P[dPPCS]) construct suppressed the occurrence of multiple oocytes and egg chambers with supernumerary nurse cells (see also Table S1). (Ad) During wt oogenesis, follicle cells are mitotically (pH3Ser10 staining) active until stage 6 and subsequently proceed into endocycling [24]. At stage 5, the nurse cell chromatin has a characteristic 5-lobed appearance and at stage 6, nurse cell chromatin is completely dispersed [25,26]. Nurse cell chromatin dispersion coincides with the mitotic-to-endocycle switch (stages 6-7), during which the follicle cells of the follicular epithelium stop mitosis and initiate endoreplication. (Ae) The mitotic-to-endocycle switch is intact in dPPCS1/1 egg chambers, and no mitotically active follicle cells are observed after stage 6. (Ae-g) Examples of egg chambers in which chromosomes failed to disperse properly and in which some nuclei remained 5-lobed (arrowheads). (Ah) Example of a stage 10 dPPCS1/1 egg chamber showing 2 nurse cell nuclei that are poorly replicated and small in size. (Ai) Example of a dPPCS1/1 egg chamber with supernumerary nurse cell nuclei that are heterogenous in size. (Aj) Example of dPPCS mutant egg chambers undergoing premature apoptosis as indicated by the presence of fragmented nuclei (arrowhead). (Ak) Example of dPPCS1/1 egg chambers showing a degenerative appearance. Scale bars: 150 μm (a-c), 50 μm (d-h).

(B) Follicle cell migration and organization is disrupted in dPPCS$^{1/1}$ germaria. (Ba) Wt cysts (marked by asterisk) in region 2b adopt a lens-shape appearance (arrow marks the stalk cells). (Bb) In dPPCS1/1 germaria, the cysts (marked by asterisk) do not adopt the characteristic lens-shape appearance. Formation of the interfollicular stalk (arrow) is severely disrupted and newly formed egg chambers display features of fusion (arrowhead). (Bc) Wt follicle cells that migrate between the cysts express FasIII. When the egg chambers bud from the germarium, only the polar follicle cells (asterisk) express FasIII [7,11,27]. (oo = oocyte). (Bd) In dPPCS1/1 germaria, migration of the follicle cells is disrupted (arrow) and this results in packaging defects (7-8, 10-11), mispositioning of the oocytes (9,10,12), and induces formation of egg chambers without stalks (arrowhead). Numbers mark the oocytes. (Be-e') In wt egg chambers, Arm and DE-cad are highly expressed in the migrating follicle cells and later in the stalk cells (arrowheads) [28-30]. Asterisks mark the position of the oocytes. (Bf-f') Arm and DE-cad were abnormally expressed in dPPCS1/1 stalk cells (arrowheads). (Be") Wt germ line cells express the Vasa protein. The migrating follicle cells in region 2b adopt a convex lens-shape [31] (arrows). (Bf") dPPCS1/1 germ line cells accumulated normal amounts of Vasa, demonstrating that specification of the germ line cell was not affected. Migrating follicle cells do not exhibit a convex lens-shape (arrows). Scale bars: 20 μm.

(C) dPPCS1/1 egg chambers exhibit features of aberrant polar follicle cell and stalk cell specification. (Ca) Wt egg chambers contain two groups of polar follicle cells, one at the anterior and one at the posterior. (Cb) A dPPCS1/1 egg chamber with three groups of polar follicle cells (arrows) and a mispositioned oocyte (asterisk). (Cc) Examples of dPPCS1/1 egg chambers in which the cuboidal follicle cells are maintained in an undifferentiated state (high FasIII expression). The follicular epithelium displays a discontinuous character and the nurse cell chromatin is heterogenous in size (arrows indicate polar follicle cells). (Cd) Wt egg chambers are connected by an interfollicular stalk (arrow). (Ce) Image, obtained by making one single confocal scan, showing a dPPCS1/1 egg chamber in which the interfollicular stalk is missing (arrow). Note that the follicular epithelium appears to be a bilayer (arrowheads). (Cf) Single confocal scan showing a dPPCS1/1 egg chamber in which the follicle cells are accumulated in a bilayer at the posterior of the oocyte (arrowheads). (Cg) In dPPCS1/1 ovaries, the interfollicular stalks are sometimes elongated and are composed of undifferentiated follicle cells (arrowhead). Arrows mark two groups of polar follicle cells in the adjacent egg chamber. Scale bars: 50 !m (c), 20 !m (a, b, d-g).

(D) Notch localization is disrupted in dPPCS$^{1/1}$ germaria. Formation of the stalk and the polar cells depends on a Delta-Notch signaling route that specifies the anterior polar follicle cells, which in turn induce stalk cell formation [12,32]. Abnormal follicle cell differentiation, multiple layering and aberrant packaging have been observed in Notch mutant females [7,11,12,22,33]. (Da-a") In wt germaria, Notch is highly expressed in region

2b, while Notch localizes cortically in newly produced egg chambers [33]. (Db-b") In dPPCS1/1 germaria, protein levels of Notch were frequently lower/abnormal (40%; n=20 germaria) compared with wt germaria (arrowheads). In a fused egg chamber, Notch localization at the cortical membrane was not disrupted. At the posterior half of this egg chamber low levels of FasIII were observed, while at the anterior half high levels of FasIII were visible using antibody staining, indicating that differentiation of the cuboidal follicle cells was not affected (arrows indicate polar follicle cells) Scale bars: 20 μm.

(E) dPPCS$^{1/1}$ egg chambers and germaria are apoptotic. Wt and dPPCS1/1 ovaries were investigated for apoptosis 144 h AE. (Ea) Under normal physiological conditions apoptosis is initiated during cytoplasmic dumping (stage 10). During stage 10, the nurse cell nuclei of wt egg chambers were positive for TUNEL staining (no staining was observed in <stage 9 egg chambers). (Eb-d) The follicle cells that surround the dPPCS1/1 germaria and egg chambers are positive for TUNEL staining, indicating that the somatically derived follicle cells were undergoing apoptosis. Although TUNEL positive nurse cells were also observed, apoptosis was most profound in the follicle cells. (Ed) Quantification of the percentage of ovariols with apoptotic egg chambers. Numbers depicted at the top of each histogram represents the number of ovarioles. Scale bars: 100 μm

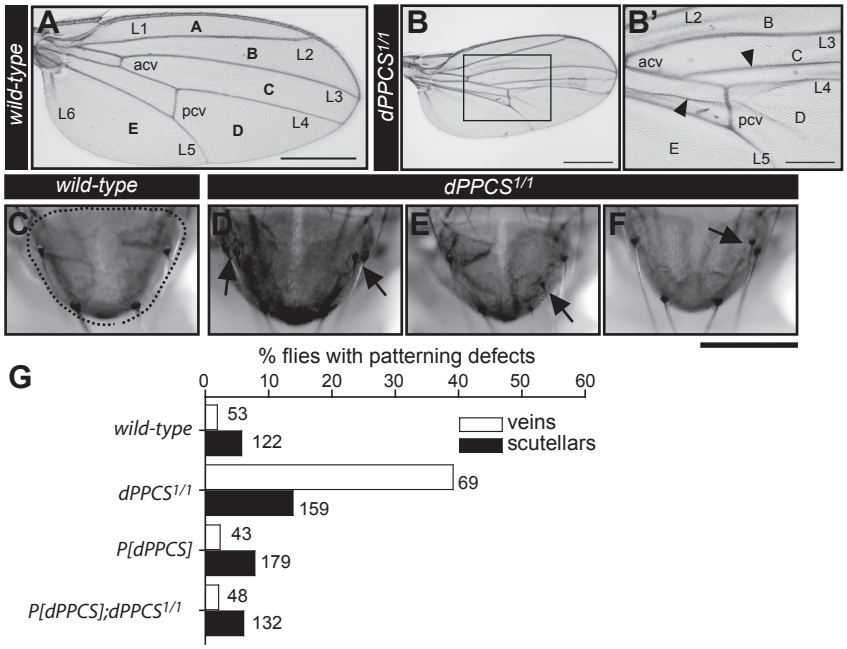

Figure S2. Mutations in *de novo* CoA biosynthesis affect wing vein and scutellar patterning

Wing vein and scutellar patterning was analyzed in dPPCS1/1 and wt. (A) Dorsal wing surface of wt. (L1-L6: longitudinal veins 1 to 6; acv: anterior cross veins; and pcv: posterior cross veins) A-E (intervein sectors). (B-B') dPPCS1/1 wings displayed ectopic veins between longitudinal veins L3-L4 and L4-L5 (arrowheads). (C) Thorax of a wt fly. The scutellum (dashed) has a pattern of four scutellars (bristles, scutellars). (D-F) Thorax of dPPCS mutant flies developed ectopic scutellars (arrows). (G) Quantification of wing and scutellar abnormalities. Numbers represent the number of flies investigated. Scale bars: 250 μm (A-B), 100 μm(B'), 500 μm (C-F).

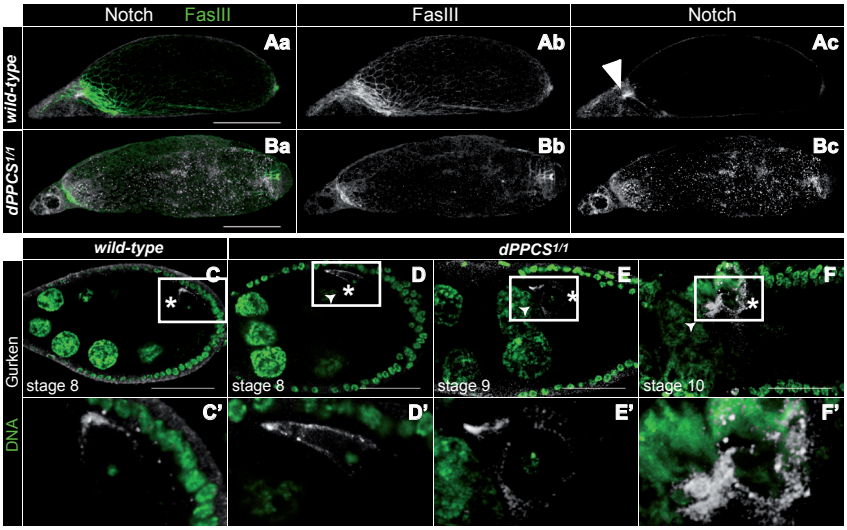

Figure S3. Notch and Grk are abnormally localized in late stage *dPPCS*$^{1/1}$ egg chambers

Wt and dPPCS1/1 ovaries were labeled with antibodies against Notch and Grk to investigate whether these signaling routes are affected in dPPCS mutant egg chambers. DAPI was used to visualize DNA. (Aa-c) A wt egg chamber at stage 13. The FasIII positive cells are producing the dorsal appendages and the operculum. Notch localization is restricted to the anterior follicle cells (arrowhead). (Ba-c) In dPPCS mutant stage 13 egg chambers, FasIII localization was abnormal, dorsal appendage and operculum formation was disrupted, and Notch was localized throughout the entire follicular epithelium. (C-F) Images obtained with single confocal scans of wt (C) and dPPCS1/1 (D-F) egg chambers. (C) The Grk protein localizes at the dorsoanterior corner of the oocyte in wt stage 8-9 egg chambers. (D-F) Grk localization was present in dPPCS1/1 mutant egg chambers, but the protein was frequently abnormally localized along the dorsoanterior corner in stages 8-9, most likely due to the disrupted shape of this corner (D) and progressively worsened when egg chambers proceeded into late stage oogenesis (stages 10-11) (E-F). The nurse cell nuclei are in close proximity to the dorsoanterior corner, indicating that these nuclei were not properly anchored during dumping (arrowheads). Note that the follicular epithelium appears disorganized. Asterisks mark the position of the oocyte. Scale bars: 150 μm (A-B), 50 μm(C-F).

Figure S4. Mutations in the *de novo* CoA biosynthesis route affect morphogenesis

Like dPPCS1/1 females, dPANK and dPPAT-DPCK (NB: in Drosophila the dPPAT and dDPCK enzymes are encoded by one gene and translated into one bifunctional enzyme) mutant females have fertility defects. The dPANK1, P[dPANK] and dPPAT-DPCK43 lines have been previously described [1]. Females that carry a mutation in the dPANK gene did not deposit eggs, while the dPPAT-DPCK43/43 females deposited 0.36 ± 0.04 eggs/24 h, of which 20.1% (n=232) were able to hatch. (A) dPANK1/1 ovaries dissected 48 h AE are poorly developed and do not contain eggs. (B) Five-d-old dPANK1/1 ovaries contained eggs, which are all small, ball-shaped and contain short dorsal appendages. This phenotype is identical to the eggs found in myospheroid [34], Dlar [35,36], kugelei [37], dystroglycan [38,39] and quail [40]. All of these genes encode proteins that are required for proper F-actin dynamics. Small ball-shaped eggs are typically due to loss of actin regulatory elements that control the polarized arrangement of F-actin fibers at the basal cortex of all follicle cells. During stages 5-8, these F-actin arrays are arranged in such a way that the fibers run perpendicular to the anteroposterior axis of the egg chamber and give the egg chamber a planar polarity that is required to create elongated eggs [23,41,42]. (C-C') In dPANK1/1 wings, anterior cross vein (acv) and posterior cross vein (pcv) formation was incomplete (arrowheads) and mispositioned cross veins between L2 and L3 were found (boxed arrowhead). (D) dPPAT-DPCK43/43 ovaries dissected 48 h AE are poorly developed and do not contain eggs. (E) 17% of the eggs from

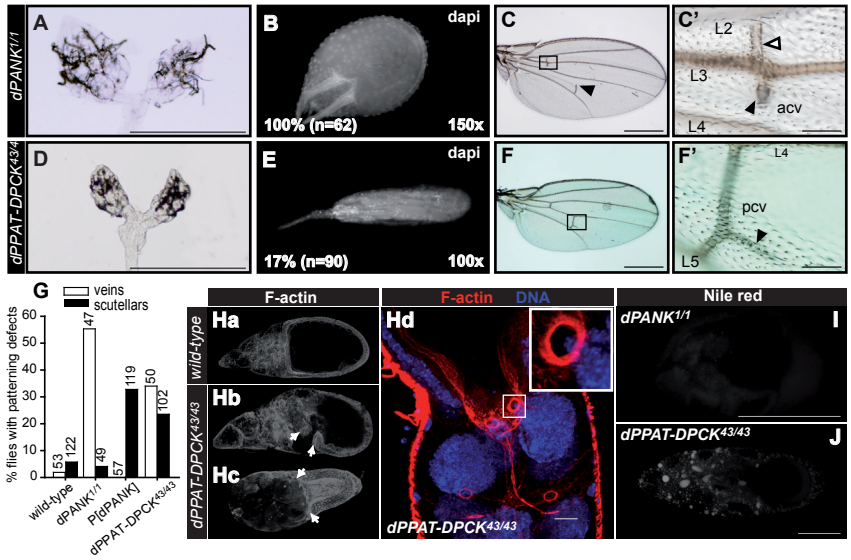

5-d-old dPPAT-DPCK43/43 females were elongated along the anteroposterior axis and exhibited a collapsed phenotype. (F-F') In dPPAT-DPCK43/43 wings, ectopic vein formation initiated from the posterior cross vein (arrowhead). (G) Quantification of wing and scutellar abnormalities in dPANK1/1 and dPPATDPCK43/ 43 flies. Numbers represent the number of flies investigated. dPANK1/1 flies did not develop ectopic macrochaetae; however, in flies that carried a FLAG-tagged dPANK cDNA under the control of an ubiquitin promoter (P[dPANK]) [1], an increase in the formation of macrochaetae was found, suggesting that dPANK overexpression induced the formation of ectopic scutellars. (H) Wt (Ha) and dPPAT-DPCK43/43 (Hb-Hd) ovaries were stained with rhodamin-phalloidin to visualize the F-actin network during cytoplasmic dumping. DAPI was used to visualize DNA. (Hb-Hc) Cytoplasmic dumping and centripetal migration of the follicle cells (arrows) was frequently severely disrupted in dPPAT-DPCK43/43 egg chambers. (Hd) Likely as a result of aberrant Factin assembly, we frequently found ring canals plugged with nurse cell nuclei in dPPAT-DPCK mutant egg chambers, suggesting that aberrant dumping underlies the production of long elongated eggs as observed in E. (I) Production of neutral lipids (Nile red staining) was hardly detected in dPANK1/1 egg chambers. (J) Production of neutral lipids (Nile red staining) and transport of lipid droplets to the oocyte was disrupted during oogenesis in dPPAT-DPCK mutants. Although levels of neutral lipids were not severely affected in dPPAT-DPCK43/43 mutants, abnormal large lipid droplets were observed, indicating that lipid droplet formation was impaired [43] (compare Fig. 3A). Scale bars: 500 µm (A,D), 250 µm (C, F), 50 µm (C', F'), 100 µm (Ha-Hc, I, J), 20 µm (Hd)